Supporting Information

Yu et al. 10.1073/pnas.1309085110

SI Materials and Methods

Cell Culture, Plasmids, Antibodies, and Chemicals. Primary human lung fibroblasts LF1, BAP1-deficient human lung squamous carcinoma NCI-H226, cervical cancer HeLa, osteosarcoma U2OS, breast cancer MCF7 carrying an I-SceI cassette, and HEK293T cells were cultured in DMEM supplemented with 10% (vol/vol) FBS and penicillin/streptomycin (Pen/Strep) in 5% CO_2 at 37 °C. Chicken bursa lymphoma DT40 Cre-1 (1) was cultured in Roswell Park Memorial Institute medium supplemented with 10% FBS, 1% chicken serum, 100 μM β-mercaptoethanol, and Pen/Strep in 5% CO_2 at 40 °C. Cervical cancer HeLa S3 cells used for complex purification were cultured in Minimum Essential Media supplemented with 5% (vol/vol) FBS and Pen/Strep in 5% CO_2 at 37 °C.

Cloning of human *BAP1* WT and C91S was described (2). BAP1 mutant in phosphorylation sites [phosphomutant (P-MUT): T273A, S276A, S571A, S583A, S592A, and S597A] was generated using gene synthesis (BioBasic). Other mutants of BAP1 were generated by site-directed mutagenesis. BAP1 (WT and mutants) were then subcloned into pENTR D-Topo plasmid (Life Technologies) and recombined into pMSCV-Flag/HA-IRES-Puro. The targeted sequences of shBAP1 #1 and #2 are GGCTGAGATTGCAAACTATGAG and GGTTTCAGCCCTGAGAGCAAAG, respectively (2). pCDNA.3 Flag-H2A plasmid was described (3).

Monoclonal anti-BAP1 (C4), polyclonal anti-BAP1 (H300), monoclonal anti-BRCA1 (D9), polyclonal anti-RAD51 (D92), polyclonal anti-53BP1 (H300), polyclonal anti-YY1 (H414), monoclonal anti-p53 (DO.1), and polyclonal anti-OGT (H300) antibodies were purchased from Santa Cruz. Polyclonal anti-ubiquityl-histone H2A lysine 119 (8240), polyclonal antiphosphohistone H3 serine 10 (3377), anti-pSQ/TQ (G) (6966), pCHK1 S345 (2348), and normal rabbit IgG (2729) are from Cell Signaling. Monoclonal antiphospho-H2A.X serine 139 (05-636) and monoclonal anti–β-actin (C4) antibodies were purchased from Millipore. Polyclonal anti–HCF-1 (A301-400A) and polyclonal anti-ASXL2 (A302-037A) were purchased from Bethyl Laboratories. Monoclonal anti-Flag (M2) was purchased from Sigma, and monoclonal anti-HA (HA11) was purchased from Covance. Polyclonal antiphospho–DNA-PK S2056 (ab18192) is from Abcam. Mouse polyclonal anti-FOXK1 antibody was provided by Xiao-Hua Li (Southwestern University of Texas, Dallas, Texas). Fluorophore-coupled secondary antibodies anti-mouse/anti-rabbit Alexa Fluor 488 and Alexa Fluor 596 were purchased from Life Technologies. The PI3K inhibitor caffeine (4) was purchased from Sigma-Aldrich. The ATM inhibitor KU-55933 (5) was purchased from Selleck Chemicals. The ATR inhibitor VE-821 (6) was purchased from Selleck Chemicals. The CDK1 inhibitor RO-3306 (7) was purchased from Calbiochem. The CDK1, -2, and -5 inhibitor Roscovitine (8) was purchased from Cell Signaling. The CDK2 inhibitor Purvalanol A (9) and GW8510 (10) were purchased from Abcam and Sigma-Aldrich, respectively. The CDK2, -1, and -4 inhibitor SU9516 (11) was purchased from Tocris Bioscience.

Small Interfering RNA Deubiquitinases Screen. U2OS cells were transfected with individual siRNA pool (consisting of four pooled siRNA oligonucleotides) targeting deubiquitinases (DUBs; ON-TARGETplus SMARTpool siRNA Library—Human Deubiquitinating Enzymes) or the nontarget control from Dharmacon (G-104705; Lot 10138) using Lipofectamine 2000 (Life Technologies); 3 d posttransfection, cells were exposed to 5 Gy ionizing radiation (IR) and collected 24 h later for immunostaining. Approximately 100 cells were counted for each condition, and cells with more than 10 DNA damage foci were considered as positives.

RNAi and Immunoblotting. For siRNA experiments, we used ON-TARGETplus SMARTpool siRNA against human BAP1 and nontarget control (Dharmacon). Transfections of siRNA or shRNA constructs were done using Lipofectamine 2000 (Life Technologies).

Total cell extracts were prepared in lysis buffer (25 mM Tris·HCl, 1% SDS), and protein concentration was determined by bicinchoninic acid assay. SDS/PAGE and Western blotting were conducted according to standard procedures. The band signals were acquired using the LAS-3000 LCD camera coupled to the MultiGauge software (Fuji).

BAP1 Gene Targeting. The DT40 Cre-1 cell line harboring the fusion protein of Cre and the hormone binding domain of the mutated estrogen receptor (1) was used to generate the BAP1 conditional KO. Gene targeting and Southern blotting were done essentially as previously described (12). The targeting constructs were assembled in pBluescript II. The first BAP1 allele was targeted with a puromycin resistance cassette. The second allele was replaced by an insert flanked with two loxP sites that contained the human *BAP1* gene under the chicken β-actin promoter and a blasticidin S-resistance cassette. Antibiotic resistance cassettes were previously described (1). Positive clones were screened by Southern blot on BglII-digested genomic DNA with probes generated by PCR with the following primers: TCCCGCTCAACTGAAGTTCT and CCACAAATGCTCTGAGTGGA. To excise the human *BAP1* gene from the conditional BAP1 KO cells, cells were treated with 50 nM 4-hydroxytamoxifen for 4 d. Cells were then subcloned to isolate BAP1 constitutive KO clones.

Clonogenic Survival Assay. DT40 cells were seeded on plates containing DMEM with 1.5% (vol/vol) methylcellulose, 10% (vol/vol) FBS, 1% chicken serum, 100 μM β-mercaptoethanol, and Pen/Strep. For the IR treatment, the cells were exposed to a cesium-137 source (Gamma Cell; Atomic Energy Canada) at the indicated doses before seeding. For the Olaparib treatment, cells were seeded in the methylcellulose media containing the indicated concentrations of Olaparib (Selleck Chemical). Cells were incubated at 40 °C for 20–30 d to allow colony formation.

H226 stable cell lines expressing Flag-HA-BAP1 WT or mutant forms were treated with indicated doses of IR and incubated for 5–7 d. The surviving colonies were washed with PBS and fixed with 3% (wt/vol) paraformaldehyde for 20 min. Cells were then stained with 0.2% crystal violet for 10 min followed by several washes with PBS. Retained staining was then extracted with 10% acetic acid, and the OD of the extracted dye was determined by spectrophotometry at 540 nm. The population survival rate is determined by the average ratio between the OD of the treated sample and the untreated control sample.

Chromosome Aberrations Analysis. DT40 cells were treated with 2 Gy IR and fixed after 3.5 h. To enrich cells in metaphase, cells were treated with 100 ng/mL colcemid for 2 h before fixation, metaphase spreading, and Giemsa staining. Analysis was performed on 100 metaphases of each population. Chromosome abnormalities (isochromatid/chromatid gaps and breaks and radial figures) were scored.

Surface IgM Phenotype Conversion Assay. After 20 min of incubation with anti-chicken IgM-FITC (1:800; A30-102F; Bethyl) in PBS containing 2% BSA, DT40 cells were sorted by flow cytometry to obtain homogeneous surface IgM− populations. Multiple cell populations were cultured in 24-well plates (100,000 cells/well) for 90 doubling times (splitting 1:2 every 1 or 2 d). Their surface IgM phenotype is determined by flow cytometry with the same staining procedure used for cell sorting.

Immunofluorescence. Cells were immunostained as previously described (2). The nuclei were stained with DAPI. Images were acquired using the Zeiss Axio Imager Z.2 microscope, Zeiss Acroplan/N-Acroplan 40×/0.65–0.17 objective, and AxioCAM MRm camera.

Flow Cytometry Analysis. DNA content of cells was analyzed essentially as described (13). Briefly, cells were harvested by trypsinization and fixed with 70% (vol/vol) ethanol. After PBS wash, cells were treated with 100 μg/mL RNase A for 30 min at 37 °C and stained with 50 μg/mL propidium iodide.

DT40 cells intracellular staining for anti-BAP1 (monoclonal) and antiphosphohistone H3 serine 10 was done as follows. Around 1×10^6 cells were fixed with 70% (vol/vol) of ethanol, blocked with 1% BSA in PBS, and incubated with the indicated primary antibody for 1.5 h followed by incubation with Alexa Fluor 488-coupled secondary antibody for 1 h. Between the antibodies incubation, cells were washed with PBS and PBS containing 1% BSA. DNA was costained as described above.

BrdU incorporation in DT40 cells was determined using 1×10^6 fixed cells after incubation with 20 μM BrdU for 30 min. DNA of the fixed cells was denatured using HCl 4N/Triton 0.5% for 30 min and neutralized by 100 mM Borax, pH 8.5. Cells were then blocked with 1% BSA in PBS followed by incubation with anti-BrdU antibody coupled to Alexa 488 (1:200; clone MoBU-1; Life Technologies) for 1 h. DNA was costained as described above.

Cells were analyzed using an LSRII flow cytometer (Becton Dickinson), and data were processed with FlowJo V887 software (Tree Star, Inc.).

ChIP on I-SceI–Induced Double-Strand Break. Induction of a single double-strand break after I-SceI expression, ChIP experiments, and real-time PCR were done essentially as previously described (14). Polyclonal anti-BAP1 (H300), polyclonal antiubiquitinated histone H2A lysine 119 (DC27C4), and normal rabbit IgG (2729) were used for ChIP experiments. Primers for ChIP experiments were described earlier (15). ChIP on ectopically expressed Flag-HA-BAP1 or mutants was conducted using anti-Flag antibody. BAP1 constructs were first transfected using X-tremeGENE 9 (06365779001; Roche) and then, electroporated 24 h later with the pCAG-ISCEI plasmid before harvesting. Values were calculated as a percentage of the input relative to the IgG control, which is set to one.

Chromatin Fractionation. Chromatin fraction was obtained as previously described (16). Briefly, HeLa cells were treated with 15 Gy IR and fractionated with 50 mM Tris·HCl, pH 7.3, 50 mM NaCl, 0.5% Triton, 5 mM EDTA, 50 mM NaF, 10 mM β-glycerophosphate, 1 mM Na_3VO_4, 10 mM 2-mercaptoethanol, 1 mM PMSF, and antiprotease mixture (Sigma). The pellet fraction (the chromatin) was washed several times with the fractionation buffer before sonication. Proteins were quantified and used for Western blotting.

Purification of BAP1-Associated Proteins After DNA Damage and Identification of Phosphorylation Sites. Around 3×10^9 HeLa S3 cells expressing stably Flag-HA-BAP1 or the empty vector (2) were treated with 10 Gy IR. Total extracts were prepared 3 h posttreatment by lysing cells with 50 mM Tris·HCl, pH 7.3, 50 mM NaCl, 0.5% Nonidet P-40, 50 mM NaF, 10 mM β-glycerophosphate, 1 mM Na_3VO_4, 10 mM 2-mercaptoethanol, 1 mM PMSF, and antiprotease mixture (Sigma). Lysates were clarified by centrifugation at $20,000 \times g$ for 30 min and filtration through a 0.45-μM filter. Tandem purification (Flag-HA) was done essentially as previously described (17). MS analysis was provided by the Taplin Facility at Harvard Medical School. PRO-Q Diamond phosphoprotein gel stain was purchased from Life Technologies. The polyacrylamide gel was fixed and stained according to the manufacturer's protocol.

Ubiquitin-Vinyl Methyl Ester Hybridization Assay. Ubiquitin-Vinyl Methyl Ester probe purification and hybridization assay were done as previously described (18). Purified BAP1 complexes or total cell extract were incubated with Ubiquitin-Vinyl Methyl Ester for 2 h at room temperature. Reactions were stopped by adding Laemmli buffer and analyzed by Western blotting.

In Vitro ubH2A Deubiquitination Assay. Native nucleosomes were isolated from HEK293T cells transfected with pCDNA.3 Flag-H2A. As previously described with some modifications, soluble chromatin fraction was obtained by nucleosomes digestion with micrococcal nuclease (MNase; Sigma) (19). Cells were lysed in 420 buffer (50 mM Tris·HCl, pH 7.3, 420 mM NaCl, 1% Nonidet P-40, 1 mM PMSF, protease inhibitor mixture; Sigma) and 20 mM *N*-ethylmaleimide (NEM) to block any DUB activity associated with chromatin. After centrifugation, the chromatin pellet was washed two times with the same buffer followed by two washes using MNase buffer (20 mM Tris·HCl, pH 7.3, 100 mM KCl, 2 mM $MgCl_2$, 1 mM $CaCl_2$, 0.3 M sucrose, 0.1% Nonidet P-40, 1 mM PMSF, protease inhibitor mixture). Chromatin was then treated with 3 U/mL MNase for 10 min at room temperature, and the reaction was stopped with 5 mM EDTA. After high-speed centrifugation, the soluble chromatin fraction was incubated overnight at 4 °C with Flag M2 agarose beads (Sigma). Beads were then washed several times with EB 300 buffer [50 mM Tris·HCl, pH 7.3, 5 mM EDTA, 300 mM NaCl, 10 mM NaF, 1% Nonidet P-40, 1 mM PMSF, 1 mM DTT, and protease inhibitors mixture (Sigma)] containing 20 mM NEM followed by several washes with EB 300 buffer without NEM. Bead-bound nucleosomes were then eluted with Flag peptides (0.2 μg/mL). The isolated nucleosomes were used for the in vitro deubiquitination assay with Flag-HA BAP1 complexes purified at different times after IR treatment (5 Gy). The DUB reaction was carried in 50 mM Tris·HCl, pH 7.3, 1 mM $MgCl_2$, 50 mM NaCl, and 1 mM DTT for 4 h at 37 °C, stopped by adding 2× Laemmli buffer, and analyzed by Western blotting.

1. Arakawa H, Lodygin D, Buerstedde JM (2001) Mutant loxP vectors for selectable marker recycle and conditional knock-outs. *BMC Biotechnol* 1:7.
2. Yu H, et al. (2010) The ubiquitin carboxyl hydrolase BAP1 forms a ternary complex with YY1 and HCF-1 and is a critical regulator of gene expression. *Mol Cell Biol* 30(21): 5071–5085.
3. Minsky N, Oren M (2004) The RING domain of Mdm2 mediates histone ubiquitylation and transcriptional repression. *Mol Cell* 16(4):631–639.
4. Sarkaria JN, et al. (1999) Inhibition of ATM and ATR kinase activities by the radiosensitizing agent, caffeine. *Cancer Res* 59(17):4375–4382.
5. Hickson I, et al. (2004) Identification and characterization of a novel and specific inhibitor of the ataxia-telangiectasia mutated kinase ATM. *Cancer Res* 64(24):9152–9159.
6. Charrier JD, et al. (2011) Discovery of potent and selective inhibitors of ataxia telangiectasia mutated and Rad3 related (ATR) protein kinase as potential anticancer agents. *J Med Chem* 54(7):2320–2330.
7. Johnson N, et al. (2009) Cdk1 participates in BRCA1-dependent S phase checkpoint control in response to DNA damage. *Mol Cell* 35(3):327–339.
8. Meijer L, et al. (1997) Biochemical and cellular effects of roscovitine, a potent and selective inhibitor of the cyclin-dependent kinases cdc2, cdk2 and cdk5. *Eur J Biochem* 243(1–2):527–536.
9. Villerbu N, Gaben AM, Redeuilh G, Mester J (2002) Cellular effects of purvalanol A: A specific inhibitor of cyclin-dependent kinase activities. *Int J Cancer* 97(6): 761–769.

10. Johnson K, et al. (2005) Inhibition of neuronal apoptosis by the cyclin-dependent kinase inhibitor GW8510: Identification of 3′ substituted indolones as a scaffold for the development of neuroprotective drugs. *J Neurochem* 93(3):538–548.
11. Lane ME, et al. (2001) A novel cdk2-selective inhibitor, SU9516, induces apoptosis in colon carcinoma cells. *Cancer Res* 61(16):6170–6177.
12. Campo VA, et al. (2013) MSH6- or PMS2-deficiency causes re-replication in DT40 B cells, but it has little effect on immunoglobulin gene conversion or on repair of AID-generated uracils. *Nucleic Acids Res* 41(5):3032–3046.
13. Affar B, et al. (2006) Essential dosage-dependent functions of the transcription factor yin yang 1 in late embryonic development and cell cycle progression. *Mol Cell Biol* 26(9):3565–3581.
14. Rodrigue A, et al. (2006) Interplay between human DNA repair proteins at a unique double-strand break in vivo. *EMBO J* 25(1):222–231.
15. Krietsch J, et al. (2012) PARP activation regulates the RNA-binding protein NONO in the DNA damage response to DNA double-strand breaks. *Nucleic Acids Res* 40(20): 10287–10301.
16. Daou S, et al. (2011) Crosstalk between O-GlcNAcylation and proteolytic cleavage regulates the host cell factor-1 maturation pathway. *Proc Natl Acad Sci USA* 108(7): 2747–2752.
17. Nakatani Y, Ogryzko V (2003) Immunoaffinity purification of mammalian protein complexes. *Methods Enzymol* 370:430–444.
18. Borodovsky A, et al. (2002) Chemistry-based functional proteomics reveals novel members of the deubiquitinating enzyme family. *Chem Biol* 9(10):1149–1159.
19. Groisman R, et al. (2003) The ubiquitin ligase activity in the DDB2 and CSA complexes is differentially regulated by the COP9 signalosome in response to DNA damage. *Cell* 113(3):357–367.

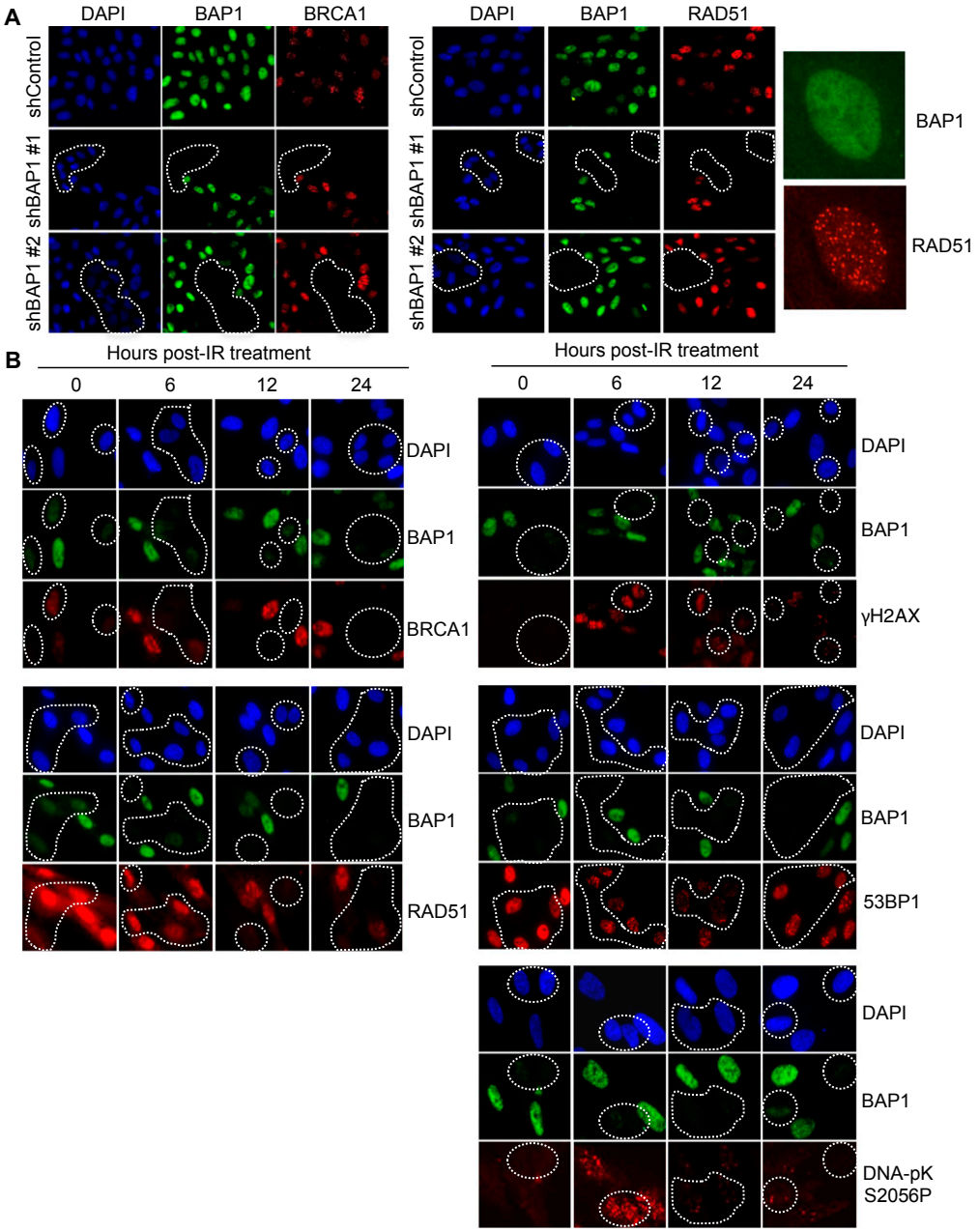

Fig. S1. (*A*) BAP1 depletion using shRNA constructs impairs IR-induced foci formation. U2OS cells were transfected with two different shRNA constructs against BAP1 (shBAP1 #1 and #2) and treated with IR (7.5 Gy); 16 h posttreatment, cells were fixed for immunostaining of the indicated proteins. Representative images of the experiment are shown. White dashed lines encircle the BAP1-depleted cells. (*B*) BAP1 promotes homologous recombination foci (BRCA1 and RAD51) formation after DNA damage. Original images of Fig. 2*A* are shown. Human fibroblast LF1 cells transfected with control or BAP1 siRNA constructs were combined (1:1) and treated with IR (7.5 Gy). Cells were fixed at different time points post-IR (0, 6, 12, and 24 h) and subjected to immunostaining of the indicated proteins. BAP1-depleted cells were identified by decreased BAP1 signal and are encircled by white dashed lines. Note that BAP1 RNAi-treated cells were mixed with the control RNAi-treated cells in these immunofluorescence experiments to facilitate the comparison.

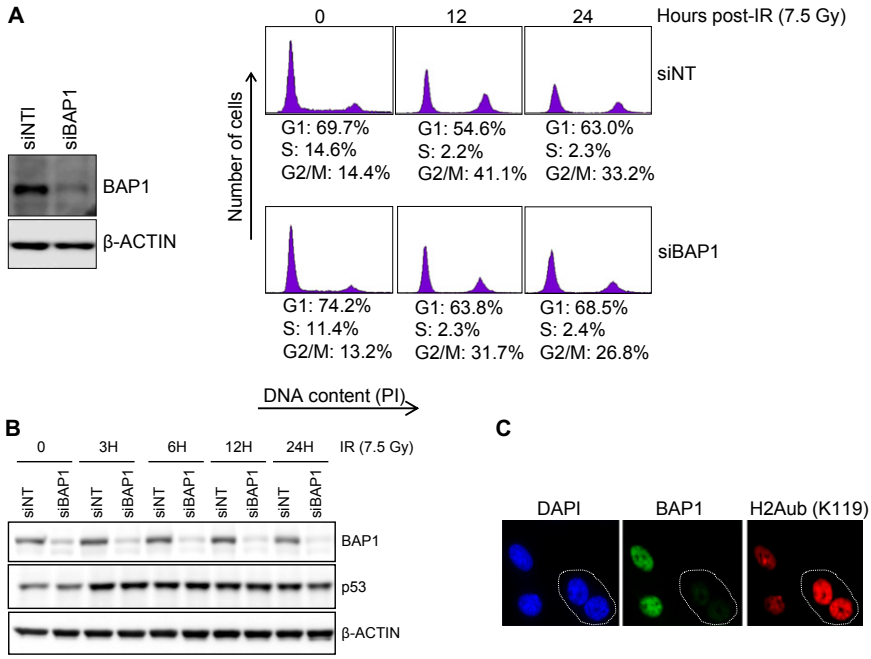

Fig. S2. (*A*) Depletion of BAP1 does not cause major defects in cell cycle. Human fibroblast LF1 cells were BAP1-depleted by siRNA and subjected for (*Left*) Western blotting of the indicated proteins and (*Right*) cell cycle profile analysis by flow cytometry using propidium iodide (PI). Percentage of cell population at each cell cycle phase (G1, S, G2/M) is shown. (*B*) Depletion of BAP1 does not induce stabilization of p53. LF1 cells were BAP1-depleted using siRNA and treated with IR (7.5 Gy). Cells were collected at different time points after IR treatment, and proteins were analyzed by Western blot for the indicated proteins. (*C*) BAP1-depleted cells have increased H2A ubiquitination. LF1 cells were treated with siNon-target control (siNT) or siBAP1 and combined (1:1) before fixation and immunostaining of the indicated proteins. Representative images of the staining are shown. BAP1-depleted cells were identified by decreased BAP1 signal and are encircled by white dashed lines. H2Aub, monoubiquitination of H2A on K119.

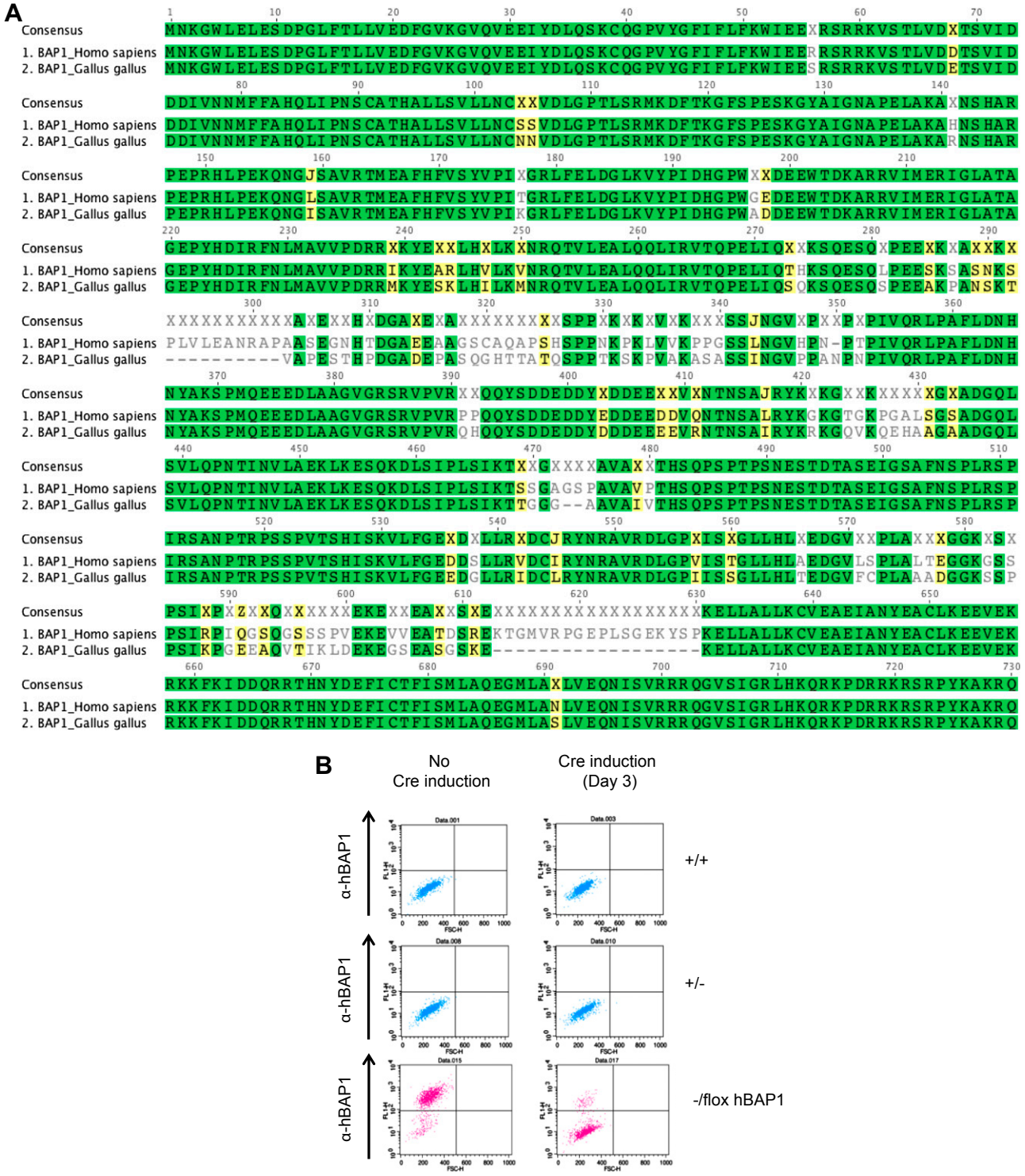

Fig. S3. (*A*) BAP1 is highly conserved between human and chicken. Alignment of *Gallus gallus* (NP_001025761.1) and *Homo sapiens* (NP_004647.1) BAP1 with ClustalW2 and visualized with Geneious software R6.1.4. Identical amino acids are highlighted in green, similar amino acids are highlighted in yellow, and not similar amino acids are in gray. (*B*) Human *BAP1* inserted in chicken *bap1* locus can be excised by Cre induction. Excision after 3 d of Cre induction was analyzed by flow cytometry using an anti-human BAP1 antibody.

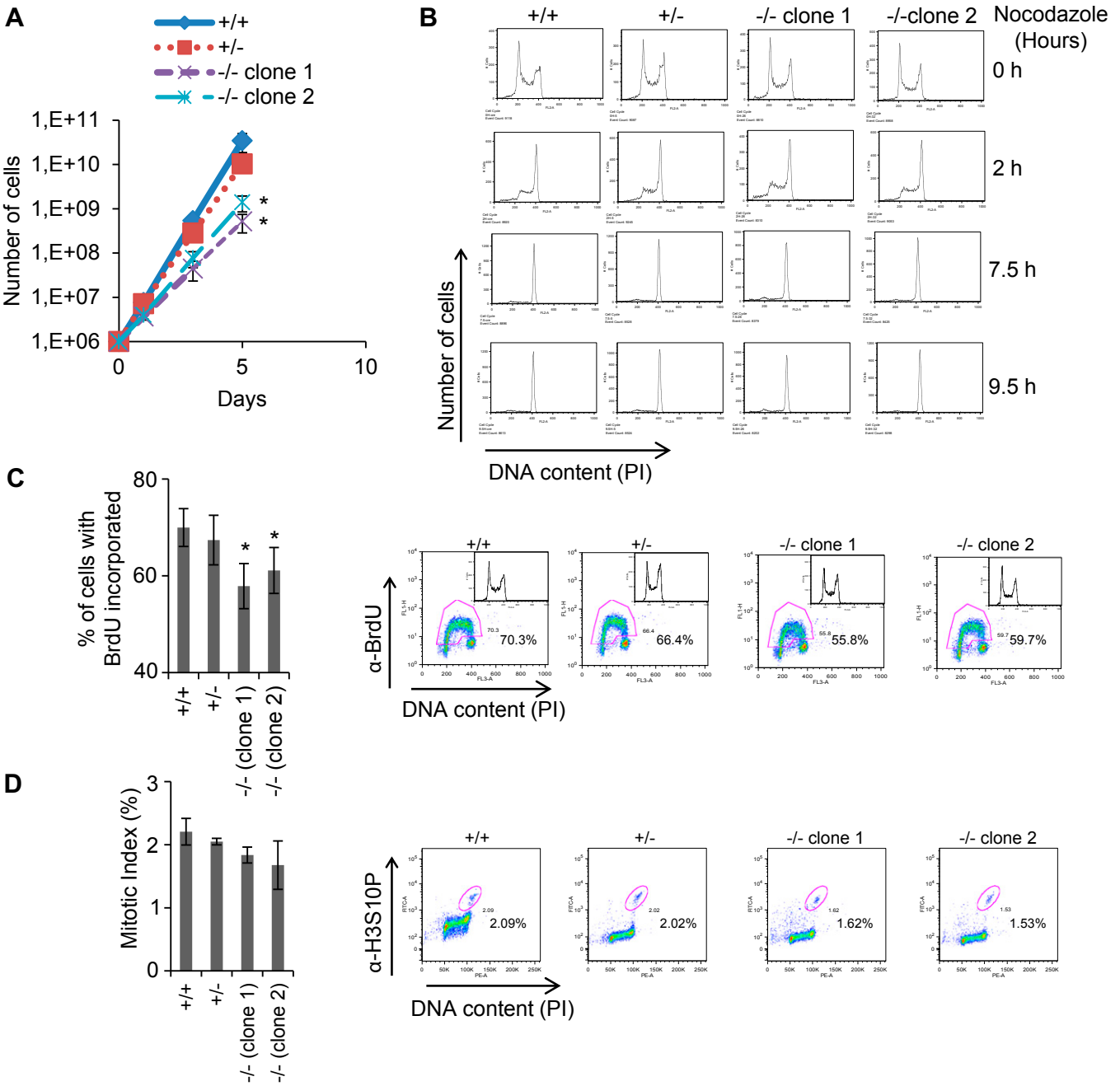

Fig. S4. (*A*) BAP1 KO cells proliferate at slower rates. Cells were seeded at the same number at day 0 and counted at days 1, 3, and 5. The experiment was repeated three times. Data are presented as mean ± SD. Statistical analysis was performed using Student *t* test. **P* < 0.05. (*B*) BAP1 KO cells did not show any major defect in G1 phase progression. BAP1 KO DT40 cells were incubated with 200 ng/mL nocodazole to arrest the cells in M phase. Different times after the addition of the drug, cells were fixed and subjected to cell cycle profile analysis by flow cytometry using PI. (*C*) BAP1 KO cells have a slightly decreased S-phase population as revealed by BrdU incorporation. Cells were incubated with BrdU for 30 min before fixation and costained with anti-BrdU antibody and PI. Cell cycle profile and BrdU uptake were analyzed by flow cytometry. The experiment was repeated three times. Data are presented as mean of BrdU-positive cells ± SD. Statistical analysis was performed using Student *t* test. **P* < 0.05. Representative results of the experiment are shown in *Right*. (*D*) BAP1 KO cells have similar number of mitotic cells than BAP1 WT cells. Asynchronous cells were fixed and costained with antiphosphorylated H3S10 antibody and PI. Mitotic population was analyzed by flow cytometry. The experiment was performed three times. Data are presented as mean of phosphorylated H3S10-positive cells ± SD. Representative results of the experiment are shown in *Right*.

A

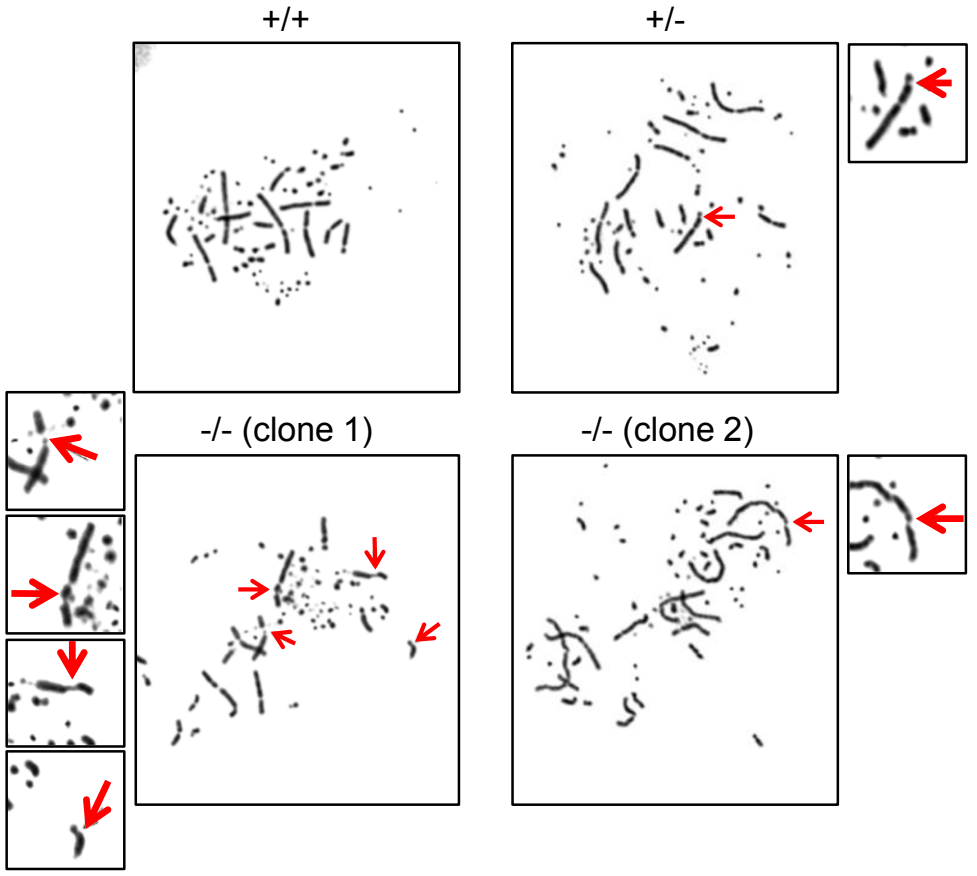

B

Genotype	Isochromatid		Chromatid		Radial figures	Total aberrations (per cell)	
	Breaks	Gaps	Breaks	Gaps		With chromatid gaps	Without chromatid gaps
+/+	(6) (0) (0)	(10) (10) (3)	(4) (9) (5)	(5) (3) (0)	(1) (0) (0)	(0.26) (0.22) (0.08)	(0.22) (0.19) (0.08)
+/-	(3) (5)	(11) (9)	(21) (38)	(8) (9)	(0) (0)	(0.43) (0.60)	(0.35) (0.51)
-/- (clone 1)	(1) (8)	(10) (26)	(25) (73)	(15) (6)	(0) (0)	(0.51) (1.15)	(0.35) (1.09)
-/- (clone 2)	(9) (2)	(21) (12)	(25) (24)	(11) (4)	(1) (0)	(0.68) (0.42)	(0.57) (0.38)

Fig. S5. BAP1 KO DT40 cells have increased chromosome breaks after DNA damage. BAP1 KO DT40 cells were treated with 2 Gy IR and fixed after 3.5 h. Colcemid was added to the cells for 2 h before fixation to enrich mitotic cells. (*A*) Representative images of metaphase spreads of each population are shown. Red arrows indicate chromosomal aberrations. (*B*) At least two independent experiments were done, and chromosome aberrations of 100 cells were counted in each experiment. Cumulative results of all experiments are shown in Fig. 3*E*.

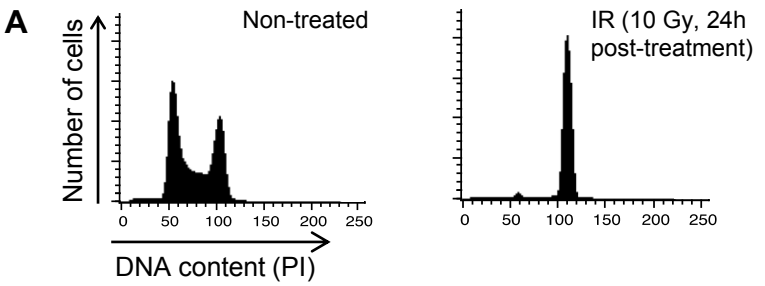

B

BAP1 Phosphorylated Peptides identified by MS after IR treatment.

Amino acid	Non Treated	IR
396	VPVRPPQQY**S#**DDEDDYEDDEEDDVQNTNSALR	VPVRPPQQY**S#**DDEDDYEDDEEDDVQNTNSALR
522	SANPTRPS**S#**PVTSHISK	SANPTRP**S#**SPVTSHISK
513	**S#**ANPTRPS**S#**PVTSHISK	**S#**ANPTRPS**S#**PVTSHISK
369	LPAFLDNHNYAK**S#**PM*QEEEDLAAGVGR	LPAFLDNHNYAK**S#**PM*QEEEDLAAGVGR
328	APAASEGNHTDGAEEAAGSCAQAPSH**S#**PPNKPK	APAASEGNHTDGAEEAAGSCAQAPSH**S#**PPNKPK
509	TSSGAGSPAVAVPTHSQPSPTPSNESTDTASEIGSAFNSPLR**S#**PIR	TSSGAGSPAVAVPTHSQPSPTPSNESTDTASEIGSAFNSPLR**S#**PIR
505	TSSGAGSPAVAVPTHSQPSPTPSNESTDTASEIGSAFN**S#**PLR	TSSGAGSPAVAVPTHSQPSPTPSNESTDTASEIGSAFN**S#**PLR
487/489	TSSGAGSPAVAVPTHSQP**S**P**T**PSNESTDTASEIGSAFNSPLR	TSSGAGSPAVAVPTHSQP**S**P**T**PSNESTDTASEIGSAFNSPLR
597	GSSPSIRPIQGSQGSS**S#**PVEK	GSSPSIRPIQGSQGSS**S#**PVEK
292	SASNK**S#**PLVLEANR	SASNK**S#**PLVLEANR
123	GF**S#**PESK	GF**S#**PESK
585	GSSP**S#**IRPIQGSQGSSSPVEK	
369	**S#**PM*QEEEDLAAGVGR	
273/276		VTQPELIQ**T**HK**S**QESQLPEESK
571		DLGPVISTGLLHLAEDGVL**S#**PLALTEGGK
592		GSSPSIRPIQG**S#**QGSSSPVEK
592/597		GSSPSIRPIQG**S#**QGSS**S#**PVEK
583/597		GS**S#**PSIRPIQGSQGSS**S#**PVEK
583		GS**S#**PSIRPIQGSQGSSSPVEK

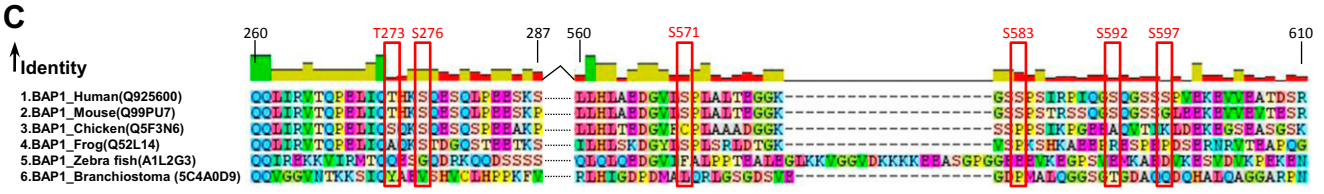

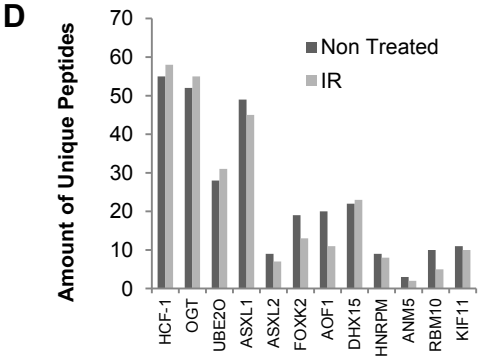

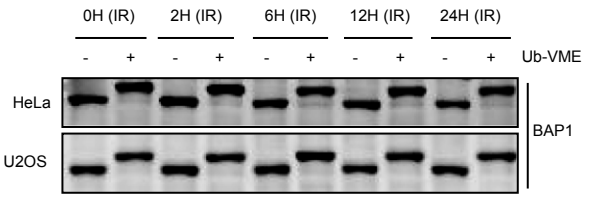

Fig. S6. Phosphorylation of BAP1 after IR treatment. (*A*) G2/M checkpoint was induced by IR treatment in the HeLa S3 cells used for BAP1 complexes purification. Cells were treated with IR (10 Gy) and fixed 24 h posttreatment for cell cycle profile analysis by flow cytometry using PI. This assay was conducted to control for the efficiency of the IR treatment in our large-scale complexes purification. (*B*) BAP1 is phosphorylated on specific residues after IR. BAP1-phosphorylated peptide sequences identified by MS are shown. Phosphoresidues are colored in red, and their positions in BAP1 sequence are indicated. (*C*) Two BAP1 IR-specific phosphosites are conserved. Alignment of BAP1 amino acid sequence from different species using Geneious software R6.1.4. Accession numbers are shown. BAP1 IR-specific phosphoresidues are squared in red. (*D*) IR treatment does not affect the assembly of major components of the BAP1 complexes. Quantification of protein peptides by MS revealed that the composition of the BAP1 core complex does not change after IR. (*E*) BAP1 DUB activity is not affected by IR. DUB activity was revealed by Ubiquitin-VME (Ub-VME) probe labeling assay. IR-treated HeLa and U2OS total cell extracts were incubated with Ub-VME probe for 2 h and analyzed by Western blot using BAP1 antibody. The shifted-up BAP1 bands are indicative of probe labeling.

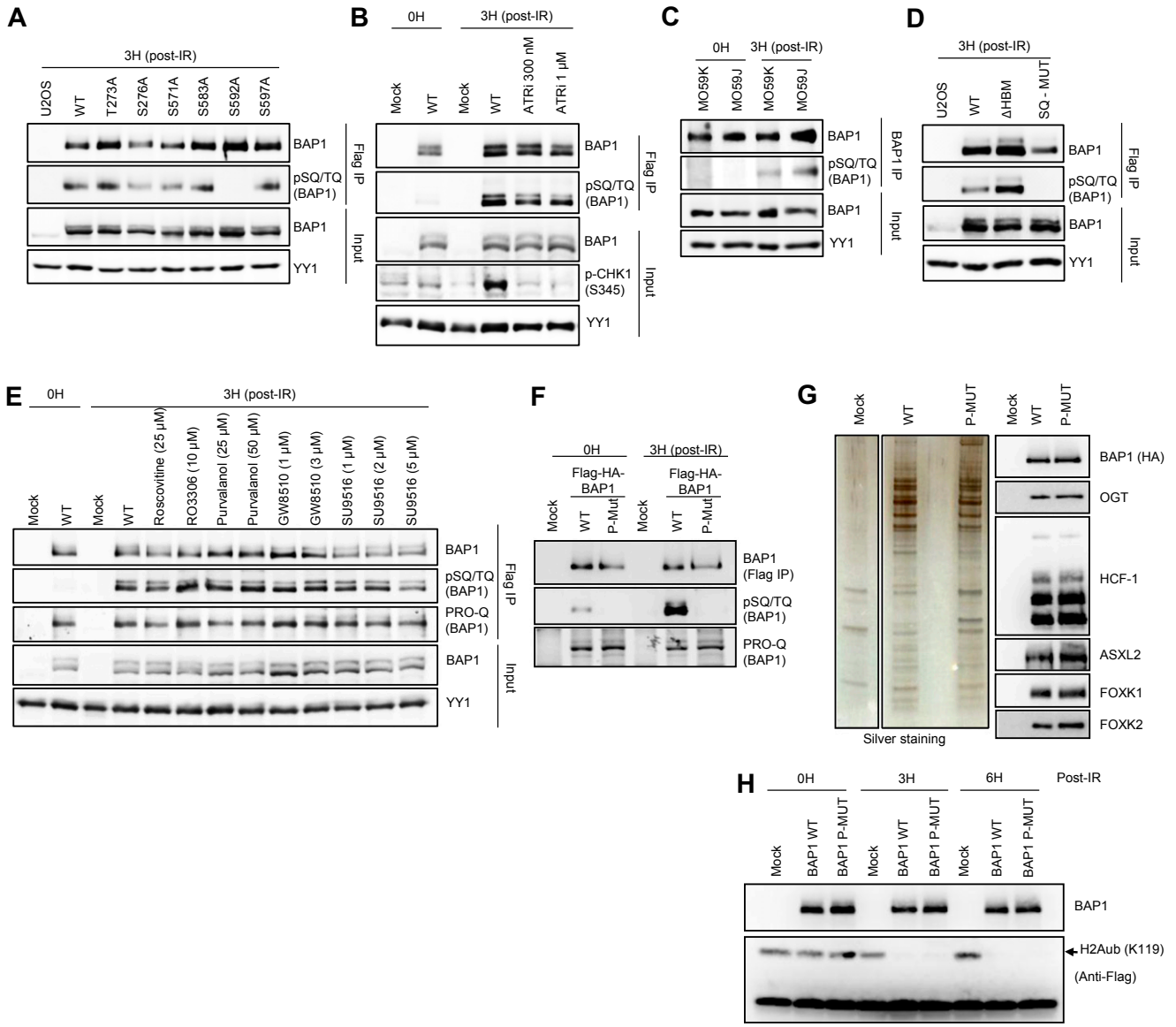

Fig. S7. Characterization of BAP1 phosphorylation after DNA damage. (*A*) Mutation of BAP1 phosphorylation sites. U2OS cells stably expressing Flag-HA-BAP1 mutants were treated with IR (7.5 Gy). Three hours posttreatment, cells were used for immunoprecipitation (IP) using anti-Flag beads. The samples were subjected to Western blotting using an anti-pSQ/TQ antibody. This antibody recognizes the pSQ motif of BAP1 at the position 592. Note that mutation of another pSQ motif, at the position 276 does not decrease the pSQ signal detected by this antibody (compared to the BAP1 signal). YY1 was used as a loading control. (*B*) The role of ATR in the phosphorylation of BAP1. HeLa cells stably expressing Flag-HA-BAP1 were pretreated with the ATR inhibitor VE-821 for 1 h before IR (7.5 Gy). Three hours posttreatment, cells were used for IP using anti-Flag beads. (*C*) DNA-PK is not required for the phosphorylation of BAP1. IP of BAP1 from DNA-PK–deficient and -proficient cells (MO59J and MO59K, respectively) before and after IR (7.5 Gy) treatment. (*D*) HCF-1 is not required for phosphorylation of BAP1. U2OS cells stably expressing Flag-HA-BAP1 WT, ΔHBM (HCF-1 binding motif), or SQ-MUT were treated with IR treatment (7.5 Gy). Three hours posttreatment, cells were used for IP of BAP1 using anti-Flag beads. (*E*) The inhibition of cyclin-dependent kinases (CDKs) does not affect BAP1 phosphorylation. HeLa cells stably expressing the empty vector or Flag-HA-BAP1 WT were pretreated with the indicated CDK inhibitors for 1 h before IR treatment (7.5 Gy). Three hours posttreatment, cells were used for IP using anti-Flag beads. The immunoprecipitated BAP1 were subjected to Western blotting using anti-pSQ/TQ antibody or stained with PRO-Q. (*F*) Characterization of BAP1 P-MUT after IR treatment. HeLa cells stably expressing the empty vector, Flag-HA-BAP1 WT, or P-MUT were treated with IR (7.5 Gy). After IP using anti-Flag beads, the samples were subjected to immunoblotting using anti-SQ/TQ antibody or stained with PRO-Q. (*G*) The BAP1 P-MUT does not lose interaction with the major partners of BAP1. HeLa S3 cells stably expressing the empty vector, Flag-HA-BAP1 WT, or P-MUT were subjected for immunopurification using anti-Flag and anti-HA beads followed by silver staining. The major components of the BAP1 complexes were detected by Western blot. (*H*) BAP1 P-MUT exhibits H2A DUB activity in vitro. Flag-HA-BAP1 WT or P-MUT complexes were incubated with purified nucleosomes for the indicated time points. H2A deubiquitination was analyzed by Western blotting.

A

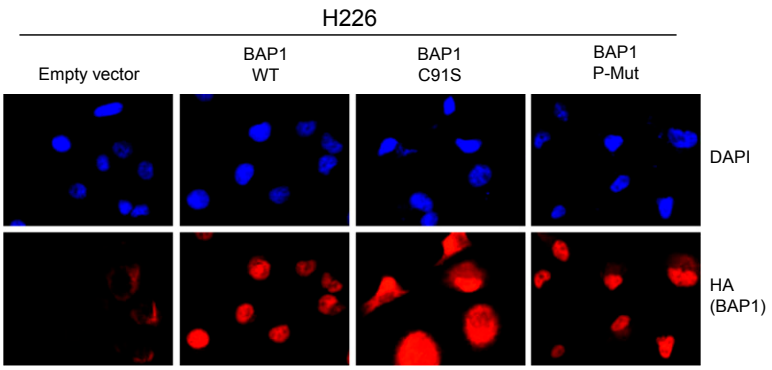

B

		%cells in Sub-G1
0H	Control	0.53
	WT	0.46
	C91S	0.25
	P-MUT	0.66
	SQ-MUT	1.83
	Delta HBM	1.41
	T273A	1.39
	S276A	3.43
	S592A	0.96
24H	Control	0.52
	WT	1.52
	C91S	0.7
	P-MUT	1.12
	SQ-MUT	2.1
	Delta HBM	0.57
	T273A	1.93
	S276A	3
	S592A	1.97
48H	Control	2.44
	WT	2.94
	C91S	3.3
	P-MUT	1.67
	SQ-MUT	2.48
	Delta HBM	2.9
	T273A	3.3
	S276A	4.65
	S592A	2.2

C

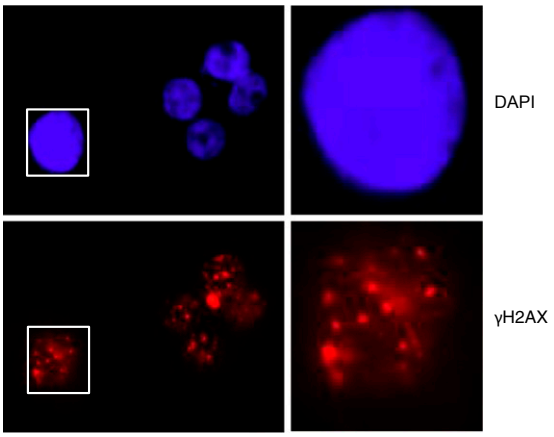

D

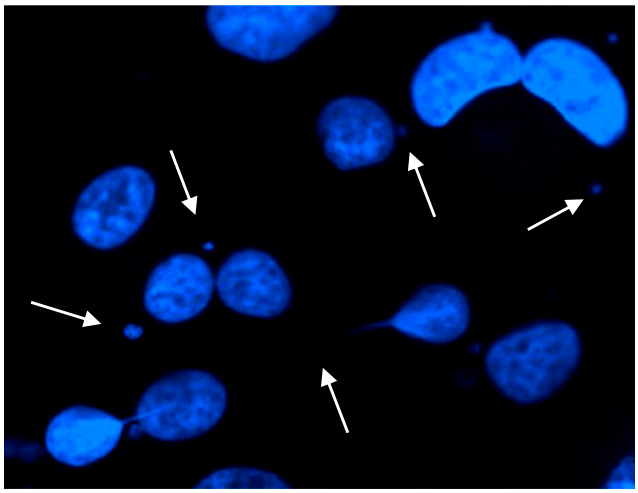

Fig. S8. H226 BAP1-deficient cells reconstituted with BAP1 WT, catalytic inactive (C91S), or P-MUT. (*A*) H226 cells stably expressing different Flag-HA-BAP1 mutants were fixed and stained with anti-HA antibody and DAPI. (*B*) Cells were treated with IR (15 Gy) and harvested at different time points posttreatment for the analysis of apoptosis. The samples were fixed with ethanol, stained with PI, and analyzed by flow cytometry for the sub-G1 population. (*C* and *D*) H226 BAP1-deficient cells harbor intrinsic DNA damage foci and exhibit genomic instability. (*C*) H226 cells were immunostained for γH2AX, and DNA was stained with DAPI. H226 cells showed constitutive γH2AX foci. (*D*) Chromosome instability in H226 cells was visualized by DAPI-stained DNA. Presence of micronuclei and internuclear bridges are indicated by the white arrows.

Table S1. List of DUBs associated with decreased or increased IR-induced foci formation

DUB name	Cells with foci (%)
BRCA1 foci*	
Control	63
BAP1	35
COPS5	41
CXORF53 (BRCC36)	38
CYLD	50
DUB3	33
OTUD5	50
OTUD7	48
PSMD14	41
SENP2	34
STAMBP	51
STAMBPL1	32
UBL5	40
UCHL1	51
UEVLD	42
USP15	53
USP3	47
USP31	33
USP6	49
C13ORF22	50
BRCA1 foci†	
Control	63
UBR1	75
UBTD1	73
USP38	75
ZRANB1	78
RAD51 foci*	
Control	51
BAP1	32
COPS5	35
DUB3	38
OTUB1	33
OTUD5	30
OTUD6B	38
PSMD14	31
STAMBP	25
STAMBPL1	23
UBL4	36
USP24	41
USP4	33
USP40	40
USP43	30
RAD51 foci†	
Control	51
UCHL1	62
USP53	61
ZRANB1	64

*Only DUBs associated with a decrease (BRCA1 foci $\leq$ 53%, RAD51 foci $\leq$ 41%) of at least 10% of cells with foci compared with the control are considered. The 10% cutoff was chosen to maximize chances of hit identification, taking into account that transfection efficiency was not determined because of lack of specific antibodies for all DUBs. Cells with more than 10 foci of the indicated protein were counted.

†Only DUBs associated with an increase (BRCA1 foci $\geq$ 73%, RAD51 foci $\geq$ 61%) of at least 10% of cells with foci compared with the control are considered. The 10% cutoff was chosen to maximize chances of hit identification, taking into account that transfection efficiency was not determined because of lack of specific antibodies for all DUBs. Cells with more than 10 foci of the indicated protein were counted.